Colloids and Surfaces B: Biointerfaces 81 (2010) 600–606

Contents lists available at ScienceDirect

Colloids and Surfaces B: Biointerfaces

journal homepage: www.elsevier.com/locate/colsurfb

Surface plasmon resonance biosensor based on Fe_3O_4/Au nanocomposites

Jian Wang, Ying Sun, Liying Wang, Xiaonan Zhu, Hanqi Zhang, Daqian Song*

College of Chemistry, Jilin University, Qianjin Street No. 2699, Changchun 130012, PR China

ARTICLE INFO

Article history:
Received 29 March 2010
Received in revised form 16 July 2010
Accepted 4 August 2010
Available online 10 August 2010

Keywords:
Core/shell structure
Fe_3O_4/Au nanocomposites
Surface plasmon resonance (SPR)
Human IgM

ABSTRACT

In this paper, the core/shell Fe_3O_4/Au nanocomposites modified with 3-mercaptopropionic acid (MPA) were prepared and applied in the surface plasmon resonance (SPR) biosensor. And the detailed investigation of Fe_3O_4/Au nanocomposites was separately performed by UV–vis spectroscopy and transmission electronic microscopy. As the magnetic property and exceptional optical properties, the Fe_3O_4/Au nanocomposites were used as the solid support for the goat anti-human IgM, which could be immobilized on the surface of SPR biosensor chip by a magnetic pillar. This novel method of immobilizing goat anti-human IgM simplified experimental procedures and facilitated the regeneration of the sensing membrane. In addition, the different diameter of Fe_3O_4/Au nanocomposites could be obtained with the different amount of MPA in the solution. And the effect of Fe_3O_4/Au nanocomposites with different diameters on the sensitivity of SPR biosensor was also explored. As a result, the SPR biosensor exhibits a satisfactory response for human IgM in the concentration range of 0.30–20.00 $\mu g\,ml^{-1}$ and the increasing nanocomposite diameter is in favor of the sensitivity enhancement of SPR biosensor.

1. Introduction

Recently, magnetic nanomaterials have proved promising applications in various fields, such as cancer diagnosis [1], drug delivery [2], biological separation and detection [3]. Due to the super paramagnetic property and high ratio of surface area to volume, magnetic nanoparticles could disperse in blood and direct to a specific target with an external magnetic field, which has great significance for medical development [4]. However, the magnetic nanoparticles are easy to aggregate and lose magnetic properties when applied in complex environmental system. And due to the lack of functional groups, the magnetic nanoparticles are difficult to couple with biomolecules directly, which limits the application of magnetic nanomaterials. These disadvantages could be improved by coating magnetic nanomaterials with metal or metal oxide shell that could protect magnetic nanomaterials and provide a platform for surface modification. Gu et al. deposited amorphous CdS on the surface of FePt nanoparticles to form a metastable core/shell structure, in which the CdS transformed into a crystalline state upon heating [5]. Xu et al. presented a facile synthesis of Au- and Ag-coated magnetic nanoparticles with controlled plasmonic and magnetic properties, and proved that the multifunctional nanoparticles have great potentials for nanoparticle-based diagnostic and therapeutic application [6]. By virtue of its exceptional optical properties, good stability and facility of surface functionality, Au was considered as an excellent material to coat magnetic nanomaterials [7]. Due to the protection of Au shell for magnetic core from oxidation, the stabilization of Fe_3O_4/Au nanocomposites (Fe_3O_4/AuNPs) was enhanced obviously. And the Au shell also provides the magnetic core with surface plasmonic properties, which makes the nanocomposites extremely interesting for optical and biomedical applications. In addition, the Au shell can be readily functionalized with thiol groups, such as 3-mercaptopropionic acid (MPA). The Au nanoparticles modified with MPA have been widely used to bind to proteins [8]. However, the Au nanoparticles have a shortcoming. When Au nanoparticles were used in the separation of proteins from a sample solution, centrifugation is generally required, which is tedious and time-consuming. The Fe_3O_4/Au nanocomposites, in which core is Fe_3O_4 and shell is Au, overcome this limit. Due to the magnetic property of Fe_3O_4, the Fe_3O_4/Au nanocomposites coupled with proteins can be separated from the sample solution easily and then immobilized on the sensing film by a magnetic pillar. In conclusion, the Fe_3O_4/Au nanocomposites combine the advantages of Fe_3O_4 and Au nanoparticles, and broaden the application of magnetic nanomaterials.

The preparation and application of Fe_3O_4/Au nanocomposites have been synthesized in several ways [9–11]. In most of the papers, Fe_3O_4/Au nanocomposites were synthesized and then the alkanethiolate was self-assembled on Au shell by immersing the nanocomposites overnight. In this paper, Fe_3O_4/Au nanocomposites modified with MPA were synthesized in one step. The MPA could be adsorbed on the surface of Au shell to control the growth of Au shell. By altering the amount of MPA, the Fe_3O_4/Au nanocomposites with different diameters were obtained [12].

* Corresponding author. Tel.: +86 431 85168399; fax: +86 431 85112355.
E-mail address: songdq@jlu.edu.cn (D. Song).

0927-7765/$ – see front matter © 2010 Elsevier B.V. All rights reserved.
doi:10.1016/j.colsurfb.2010.08.007

Surface plasmon resonance (SPR) biosensor could be applied for label-free detection of biomolecule at the metal layer surface, such as Au or Ag [13]. Owing to many advantages such as real-time, label-free and non-destructive detection, the SPR biosensor has been applied for studying various interaction partners, including proteins [14,15], nucleic acids [16], hormone [17], cells [18] and especially antigens [19]. The way of immobilizing biomolecules on the surface of biosensor chip is crucial in enhancing the sensitivity of SPR biosensor and simplifying the immunoassay procedures. The biomolecules have been immobilized on sensor surfaces by various techniques, such as sandwich assays [20,21], the interaction between avidin and biotin [22], the label of inorganic nanoparticles [13] and the chemical bond [23]. In most of these methods, proteins were immobilized on the surface of biosensor by chemical method with the binding of many chemical reagents, which is complex in the immunoassay. The magnetic nanoparticles have great advantages in the immobilization of proteins in the SPR biosensor [24]. Compared to traditional antibody immobilization on the sensing film, there is no covalent link between the biosensor chip surface and the antibody. With the magnetic property and good biocompatibility, the Fe_3O_4/Au nanocomposites could be one of the excellent candidates as carrier for protein immobilization. The conjugates of Fe_3O_4/Au nanocomposites coupled with antibody can be immobilized on the surface of the biosensor by a magnetic pillar easily. And with the exceptional optical properties, the Fe_3O_4/Au nanocomposites can play an important role in the sensitivity enhancement of the biosensor [25].

IgM is a large (950 kDa) pentamer which consists of five IgG-like monomers connected by a polypeptide chain rich in disulfide bonds and characterized by the presence of a disulfide-rich J chain. As a consequence of its pentameric structure, IgM antibodies are good in clumping microorganisms for eventual elimination from the body, and their presence in sera is a valuable indicator of running infections [26]. Therefore, rapid, accurate and sensitive analytical method for detection of IgM is important in the disease testing.

In this paper, the core/shell Fe_3O_4/Au nanocomposites modified with MPA were applied in the SPR biosensor as solid support for the goat anti-human IgM. The goat anti-human IgM was bound to Fe_3O_4/Au nanocomposites by MPA and the conjugates were immobilized on the surface of biosensor chip by magnetic pillar. Then human IgM was detected by the novel SPR biosensor. Interestingly, with the increasing amount of MPA, the thickness of Au shell deposited on the Fe_3O_4 nanoparticles decreases. By this way, the different diameter Fe_3O_4/Au nanocomposites were successfully obtained and the characteristics of nanocomposites were investigated by UV–vis and transmission electronic microscopy. And the effect of different diameter Fe_3O_4/Au nanocomposites on the sensitivity of SPR biosensor was also explored.

2. Materials and methods

2.1. Reagents

Human IgM and goat anti-human IgM (anti-human IgM) were purchased from Beijing Biosynthesis Biotechnology Company. Tetramethylammonium hydroxide (TMAOH) and 3-mercaptopropionic acid (MPA) were purchased from Jkchemical. N-hydroxysuccinimide (NHS) and 1-ethyl-3-(3-dimethylaminopropyl)carbodiimide (EDC) were purchased from Pierce. Hydrogen tetrachloroauratehydrate ($HAuCl_4{\cdot}3H_2O$) was purchased from Acrosl. Ferric chloride hexahydrate ($FeCl_3{\cdot}6H_2O$), ferrous sulfate tetrahydrate ($FeSO_4{\cdot}4H_2O$) and all other chemicals were of analytical reagent grade.

Human IgM and anti-human IgM were stored at −20 °C, and all other biological reagents were stored at 4 °C. PBS buffer (0.01 mol l^{-1}, pH 7.4) was used as running buffer.

2.2. SPR equipment

In this paper, the wavelength-modulation SPR biosensor was installed in our laboratory. It is working with Kretschmann configuration to achieve the resonant condition by attenuated total reflection (ATR) in a prism [27]. The prism was vacuum-deposited with approximately 2 nm adhesive layer of Cr and 50 nm Au film followed, which formed the biosensor chip. The light emitted from a lamp passes through the optical prism and excites surface plasmon at the interface between the biosensor chip surface and analytes. The output light is guided into the optical fiber and then enters the spectrophotometer (Ocean Optics, Inc., USA). A 2048 element charge-coupled device (CCD) linear array detector was used. A 100 μl flow cell was used for the reaction and magnetic pillar was immobilized under the optical prism. The diameter and height of the magnetic pillar are 25 and 12 mm, respectively. The sensor surface was at a distance of 13 mm from the magnetic pillar and in the magnetic field of 900 G that detected with Tesla meter.

2.3. Assay procedure

2.3.1. Preparation of Fe_3O_4/Au nanoparticles

The Fe_3O_4 nanoparticles were prepared by chemical coprecipitation methods as reported [10]. A stock solution containing $FeCl_3{\cdot}6H_2O$ (2.6 g), $FeSO_4{\cdot}4H_2O$ (1.0 g) and 12 mol l^{-1} HCl (0.425 ml) was prepared at first. Then the stock solution was dropped into 125 ml NaOH solution (1.5 mol l^{-1}) under nitrogen gas protection and vigorous stirring at 80 °C. After the reaction, the obtained Fe_3O_4 nanoparticles were washed with deionized water four times and the precipitate was dispersed in 100 ml TMAOH (0.125 mol l^{-1}) solution for further use.

The Fe_3O_4/Au nanocomposites were prepared as followed: sodium citrate (0.024 g) and a certain amount of MPA were dissolved in 100 ml water. The MPA solution should be adjusted to the neutral by adding NaOH solution. Under nitrogen gas protection and vigorous stirring, the solution was heated up to boil and 0.24 ml of Fe_3O_4 nanoparticles was added quickly. After boiling for 5 min, 0.012 mmol of $HAuCl_4$ was added immediately into the solution. The color of the solution changed from black to red, which suggests that the Au shell has been performed on the Fe_3O_4 nanoparticles successfully. After the reaction, the obtained solution was precipitated by a magnetic pillar, and the supernatant solution was removed. By this way, the pure Au nanoparticles formed can be removed. Then the solution was washed with deionized water and 5 ml of HCl (2 mol l^{-1}) was added to remove the uncoated Fe_3O_4. After the nanocomposites were washed with deionized water, the Fe_3O_4/Au nanocomposites were precipitated by a magnetic pillar and the supernatant solution was removed. 100 ml of NaOH (0.05 mol l^{-1}) was added to the precipitation and the colloid solution was obtained again. When the amounts of MPA are 0.012, 0.009, 0.006, 0.003 and 0 mmol, respectively, the Fe_3O_4/Au nanocomposites show different colors such as orange, light red, red, deep red and purple. The UV–vis absorption spectra and transmission electronic microscopy (TEM) images were used to characterize the nanocomposites.

2.3.2. Preparation of Fe_3O_4/Au nanocomposites coupled with antibody

At first, the carboxyl group of MPA on the Fe_3O_4/Au nanocomposites was activated with NHS under the catalysis of EDC for 20 min. The activated carboxyl can react to amino group of protein, while the un-activated carboxyl is hard to bind amino group at room temperature. Then 500 μl of Fe_3O_4/Au colloid solution were precipitated by a magnetic pillar and the precipitation was washed with PBS buffer solution twice. A certain concentration of goat anti-human IgM (1 ml) dissolved with PBS buffer solution was

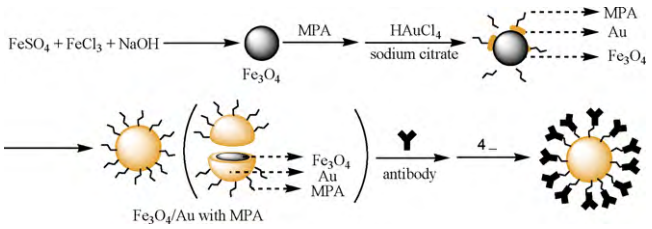

Fig. 1. Schematic diagram of the preparation of Fe_3O_4/Au nanocomposites coupled with antibody.

added into the Fe_3O_4/Au colloid solution. After 5 h, the conjugates of Fe_3O_4/Au nanocomposites coupled with anti-human IgM were obtained. Then the solution was precipitated by a magnetic pillar, and the supernatant was poured away to remove the un-reacted antibody. 1 ml PBS solution was added into the precipitation. The experimental procedures of preparing the conjugates of Fe_3O_4/Au nanocomposites coupled with anti-human IgM are shown in Fig. 1.

2.3.3. Preparation of Fe_3O_4/AuNPs/anti-human IgM sensing membrane

The conjugates of Fe_3O_4/Au nanocomposites coupled with anti-human IgM were introduced into the flow cell equipped with a magnetic pillar under the biosensor chip. The conjugates can be immobilized on the biosensor chip surface by a magnetic pillar, which greatly simplify the procedures of anti-human IgM immobilization. The immobilization of conjugates on the biosensor chip surface could produce change in refractive index profile that is observed as a shift in the SPR resonant wavelength. After 2 h, PBS buffer was injected to the flow cell to stabilize the baseline and then 1 mol l^{-1} ethanolamine hydrochloride (pH 8.0) was injected into the flow cell. As mentioned in Section 2.3.2, after the antibody added, the amino group of protein can react to activated carboxyl group of MPA. While there may be some un-reacted binding sites of activated carboxyl group, which can react to the amino group of antigen and lead to the non-specific binding of antigen. So ethanolamine hydrochloride was used to bind to the un-reacted carboxyl groups, and the non-specific binding sites on the biosensor surface can be blocked. After 10 min, PBS buffer was injected to the flow cell and the Fe_3O_4/AuNPs/anti-human IgM sensing membrane was formed.

2.3.4. Preparation of MPA/anti-human IgM sensing membrane

As a contrast, the MPA/anti-human IgM sensing membrane was also constructed. PBS buffer was used as the baseline solution, and 10 mmol l^{-1} MPA was injected into the flow cell. After 2 h, carboxyl group of MPA was activated with NHS under the catalysis of EDC for 20 min. 25.0 μg ml^{-1} anti-human IgM was injected. And the redundant anti-human IgM can be removed by PBS. 1 mol l^{-1} ethanolamine hydrochloride (pH 8.0) was used to block the non-specific binding sites on the biosensor surface. After 10 min, the MPA/anti-human IgM sensing membrane was formed.

2.3.5. Immunoassay

At room temperature, human IgM at different concentrations were separately injected into the flow cell of the SPR biosensor system. The shifts of resonant wavelength due to antibody–antigen immunoreactions were measured by SPR biosensor. After 40 min, PBS was injected into the flow cell. Then another sample solution was injected into the flow cell.

To evaluate the selectivity of the proposed method, human serum albumin and bovine serum albumin were determined by the procedure mentioned above.

2.3.6. Regeneration

After a series of human IgM immunoassays were performed, the sensing membrane of the SPR biosensor was regenerated. The magnetic pillar was taken away from the prism and water was introduced into the flow cell to wash away the Fe_3O_4/Au nanocomposite coupled with anti-human IgM.

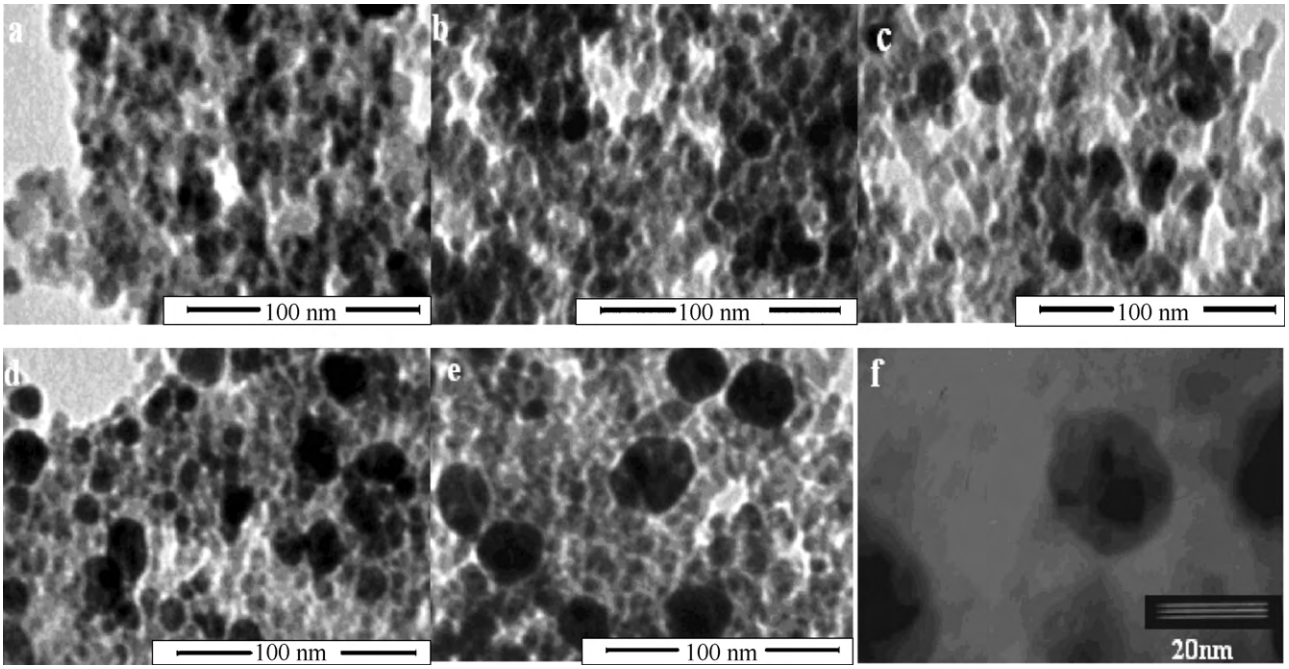

Fig. 2. TEM images of Fe_3O_4/Au nanocomposites at different diameters. (a) ~8 nm, (b) ~12 nm, (c) ~17 nm, (d) ~20 nm, (e) ~30 nm and (f) a typical 20 nm Fe_3O_4/Au nanocomposite.

3. Results and discussion

3.1. Preparation and characterization of Fe_3O_4/Au nanocomposites

Fe_3O_4 nanoparticles were first prepared as seeding materials, and then Au was deposited on the Fe_3O_4 nanoparticles in the presence of MPA to form the core/shell Fe_3O_4/Au nanocomposites. The MPA plays an important role in the synthesis of Fe_3O_4/Au nanocomposites with different diameter. As shown in Fig. 1, when the Au shell began to generate, the MPA can be adsorbed on the Au surface to restrain Au shell from growing on the Fe_3O_4 nanoparticles. So the decrease of MPA concentration in the solution results in the increase of thickness of Au shell on the Fe_3O_4 nanoparticles. Thus, the Fe_3O_4/Au nanocomposites with different diameter were obtained by adding different amounts of MPA. Fig. 2 shows the transmission electron micrographs of Fe_3O_4/Au nanocomposites with different diameter. When the amount of MPA in the solution is 0.012, 0.009, 0.006, 0.003 and 0 mmol, the diameter of Fe_3O_4/Au nanocomposites is about 8, 12, 17, 20 and 30 nm, respectively. Fig. 2f shows the transmission electron micrographs of a typical 20 nm Fe_3O_4/Au nanocomposite. The TEM images showed that there are some smaller and lighter particles, which signify bare Fe_3O_4 nanoparticles. The Au shell exhibits topographical roughness on the nanometer scale. It can be hypothesized that the Au shell grows by nucleating from small nanoparticles on the Fe_3O_4 nanoparticles surface and then develops the shell structure [28].

As the thickness of Au shell increases, the Fe_3O_4/Au nanocomposites show gradually light colors as orange, light red, red, deep red and purple. Fig. 3 shows UV–vis spectra of Fe_3O_4 nanoparticles and Fe_3O_4/Au nanocomposites with different diameter. The UV–vis spectra of Fe_3O_4 nanoparticles show that no absorption appears. When the amount of MPA added into the solution is 0.006, 0.003 and 0 mmol, Fe_3O_4/Au nanocomposites show maximum absorption at 518, 522 and 546 nm, respectively. The maximum absorption wavelength is red shifted due to the increasing diameter of Fe_3O_4/Au nanocomposites. When the amount of MPA is 0.009 and 0.012 mmol, the Au shell deposited is so thin that the absorption peaks of Fe_3O_4/Au nanocomposites are not evident.

3.2. Preparation of SPR biosensor based on Fe_3O_4/Au nanocomposites coupled with anti-human IgM

In order to select the optimal concentration of anti-human IgM to conduct the next experiment, Fe_3O_4/Au nanocomposites coupled with anti-human IgM at different concentrations were studied. The Fe_3O_4/Au nanocomposites were prepared with 0.003 mmol of MPA, and the conjugates of Fe_3O_4/Au nanocomposites coupled with anti-human IgM at different concentrations were injected into the flow cell and the conjugates can be immobilized on the biosensor chip surface by the magnetic pillar.

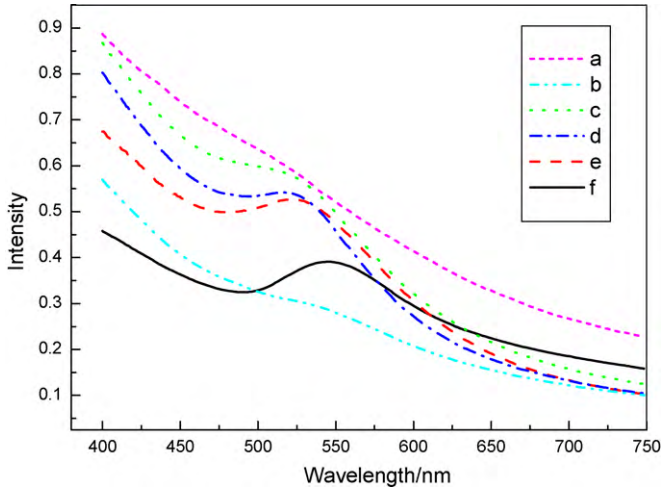

Fig. 3. UV–vis absorption spectra of Fe_3O_4 nanoparticles (a) and Fe_3O_4/Au nanocomposites at different diameters: (b) 8 nm, (c) 12 nm, (d) 17 nm, (e) 20 nm and (f) 30 nm.

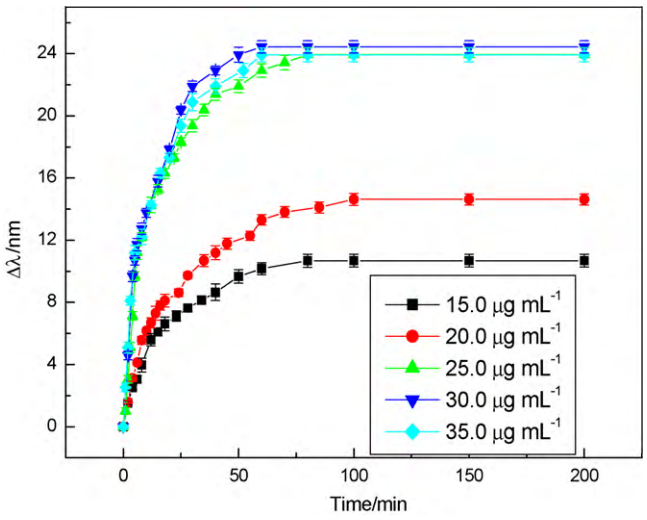

Fig. 4. The kinetic adsorption curves of Fe_3O_4/Au nanocomposites coupled with anti-human IgM at different concentrations. Error bars = ±S.D. and $n = 3$.

Fig. 4 shows the kinetic adsorption curves of immobilizing Fe_3O_4/Au nanocomposites with anti-human IgM at different concentrations. The resonant wavelength shifts significantly at first and tends to be stable in 100 min, which indicates that the immobilization of conjugates on the biosensor chip surface was completed. Due to the increase of anti-human IgM concentration, more antibodies were immobilized on the biosensor chip surface, which resulted in the resonant wavelength moving to the longer wavelength. When the concentrations of anti-human IgM are 15.0, 20.0, 25.0, 30.0 and 35.0 $\mu g\,ml^{-1}$, the shifts of resonant wavelength are 10.7, 14.6, 23.9, 23.9 and 24.4 nm, respectively (Fig. 4). With the increase of the concentration of anti-human IgM, the amount of antibody immobilized increases at first and reaches saturation gradually, which results in no change of the resonant wavelength. It means that the immobilization of anti-human IgM can reach saturation when the concentration of anti-human IgM is 25.0 $\mu g\,ml^{-1}$.

3.3. Effect of different sizes of Fe_3O_4/Au nanocomposites

In this paper, the effect of different diameters of Fe_3O_4/Au nanocomposites on the sensitivity enhancement of SPR biosensor was also studied. The conjugates of Fe_3O_4/Au nanocomposites coupled with anti-human IgM were separately injected into the flow cell. Fig. 5 shows the kinetic adsorption curves of the conjugates. It can be seen from Fig. 5, when the diameter of nanocomposite is 8, 12, 17 and 20 nm, the shifts of resonant wavelength are 16.3, 17.3, 20.3 and 23.9 nm, respectively. When the 30 nm of Fe_3O_4/Au nanocomposites coupled with anti-human IgM without MPA were immobilized on the biosensor chip surface, the corresponding maximum shift of the resonant wavelength is only 15.8 nm. In order to identify the amount of anti-human IgM immobilized, the bare Fe_3O_4/Au nanocomposites were also injected. The shifts of resonant wavelength tend to be stable in 15 min. When the diameter of nanocomposite is 8, 12, 17, 20 and 30 nm, the shifts of resonant wavelength are 0.5, 1.0, 2.3, 3.5 and 5.2 nm, respectively. The fact is not surprising that the increasing nanocomposites diameter leads to the large red-shift of resonant wavelength. With the increase

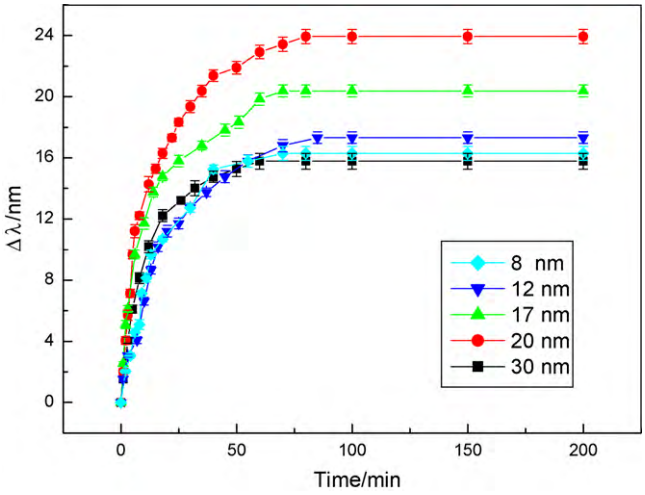

Fig. 5. The kinetic adsorption curves of conjugates of Fe_3O_4/Au nanocomposites coupled with anti-human IgM at different diameters. Error bars = ±S.D. and $n = 3$.

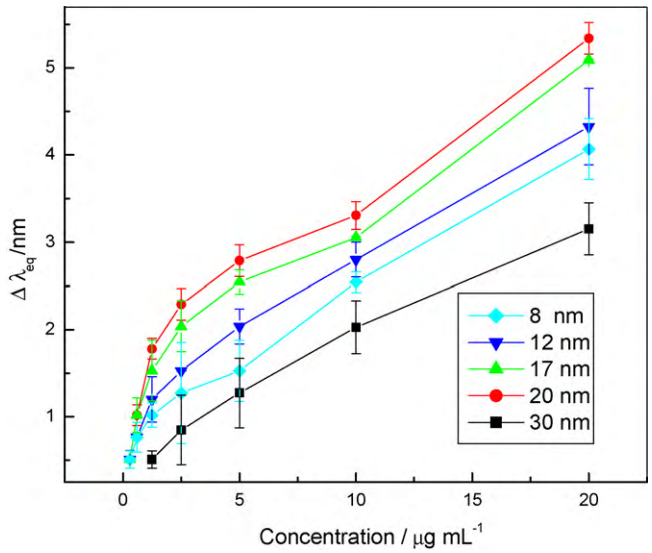

Fig. 6. The relationship between the concentration of human IgM and the shifts of the resonant wavelength ($\Delta\lambda_{eq}$) with biosensor based on Fe_3O_4/Au nanocomposites at different diameter. Error bars = ±S.D. and $n = 3$.

of Fe_3O_4/Au nanocomposites diameter, the thickness of the sensing membrane of SPR biosensor increases. SPR biosensor is highly sensitive to the minimal change of sensing membrane, which can lead to the shift of the SPR resonant wavelength [29]. As a result, it can be expected that the conjugates with larger nanocomposite immobilized on the sensing membrane, the longer shift of resonant wavelength in the SPR curve obtained. In addition, the amount of proteins immobilized on the surface of biosensor also has an important influence on the shift of the SPR resonant wavelength. The proteins can couple with Fe_3O_4/Au nanocomposites through MPA or electrostatic adherence. When there is MPA attached on the nanocomposites, the MPA can link with proteins through chemical bond, which is firm and prior to react. When there is no MPA, the Fe_3O_4/Au nanocomposites can adsorb proteins through electrostatic adherence [20], which is much weaker compared with the chemical bond between the protein and MPA. So the amount of proteins immobilized with 30 nm Fe_3O_4/Au nanocomposites is less than that immobilized with other nanocomposites. As a result, the immobilization of 20 nm Fe_3O_4/Au nanocomposites coupled with anti-human IgM leads to the largest red-shift of resonant wavelength.

Fig. 6 shows the relationship between the concentration of human IgM and the shifts of the resonant wavelength ($\Delta\lambda_{eq}$). When the Fe_3O_4/Au nanocomposites (8, 12, 17 and 20 nm) were immobilized on the biosensor chip surface, the biosensor shows a satisfactory response to human IgM in the concentration range of 0.30–20.00 μg ml^{-1} (Fig. 6). And with the increase of Fe_3O_4/Au nanocomposites diameter, the maximum shift of resonant wavelength due to antibody–antigen immunoreaction increases. The SPR biosensor shows highest sensitivity when the 20 nm Fe_3O_4/Au nanocomposites coupled with anti-human IgM was immobilized on the biosensor chip surface. As the diameter of nanocomposite immobilized in the SPR biosensor increases, the SPR curve can be expected to shift to longer wavelength, which has been proved to be beneficial to enhance the sensitivity of SPR biosensor [30]. It can also be seen from Fig. 6 that the lowest concentration that could be detected obtained by the biosensor with 30 nm nanocomposites is 1.25 μg ml^{-1}, which is 4 times higher than that obtained by the biosensor with 20 nm nanocomposites. As mentioned before, the amount of anti-human IgM immobilized with 30 nm Fe_3O_4/Au nanocomposites without MPA is less than that immobilized with other nanocomposites, which results in the low sensitivity of SPR biosensor. These results demonstrate that both the diameter of Fe_3O_4/Au nanocomposites and the amount of proteins immobilized on the sensing membrane play important roles in enhancing sensitivity of SPR biosensor. As a result, the 20 nm Fe_3O_4/Au nanocomposite that prepared with 0.003 mmol MPA is the best candidate to immobilize proteins on the surface of SPR biosensor.

3.4. Determination of human IgM

In order to study the effect of Fe_3O_4/Au nanocomposites in enhancing biosensor sensitivity, the different biosensors based on Fe_3O_4/AuNPs/anti-human IgM sensing membrane and MPA/anti-human IgM sensing membrane were constructed. The sensitivity of a biosensor chip greatly depends on the surface density of the antibodies immobilized, so it is important to select the optimum concentration of antibody. In theory, as the larger surface area of Fe_3O_4/Au nanoparticles, the needed amount of anti-human IgM immobilized by Fe_3O_4/Au nanoparticles is more than that immobilized by MPA. In order to provide enough amount for MPA/anti-human IgM sensing membrane, the same concentration of anti-human IgM was used, which can compare the sensitivity of two different biosensors effectively. So the 25.0 μg ml^{-1} anti-human IgM was used to prepare the MPA/anti-human IgM sensing membrane.

Fig. 7 shows the kinetic adsorption curves of conjugates on the biosensor and anti-human IgM on the MPA monolayer. The amount of anti-human IgM immobilized by Fe_3O_4/Au nanocomposites is significantly more than that by MPA. Fig. 8 shows the relationship between the concentration of human IgM and the shifts of resonant wavelength with the biosensor based on Fe_3O_4/Au nanocomposites and MPA. It can be seen from Fig. 8a that the SPR biosensor based on Fe_3O_4/AuNPs/anti-human IgM sensing membrane shows a good response to human IgM in the concentration range of 0.30–20.00 μg ml^{-1}. The minimum shift of resonant wavelength is 0.5 nm at 0.30 μg ml^{-1} and the maximum shift of resonant wavelength is 5.3 nm at 20.00 μg ml^{-1}. The SPR biosensor based on MPA/anti-human IgM sensing membrane shows a good response to human IgM in the concentration range of 1.25–20.00 μg ml^{-1} (Fig. 8b). The minimum shift of resonant wavelength is 0.5 nm at 1.25 μg ml^{-1} and the maximum shift of resonant wavelength is 4.1 nm at 20.00 μg ml^{-1}.

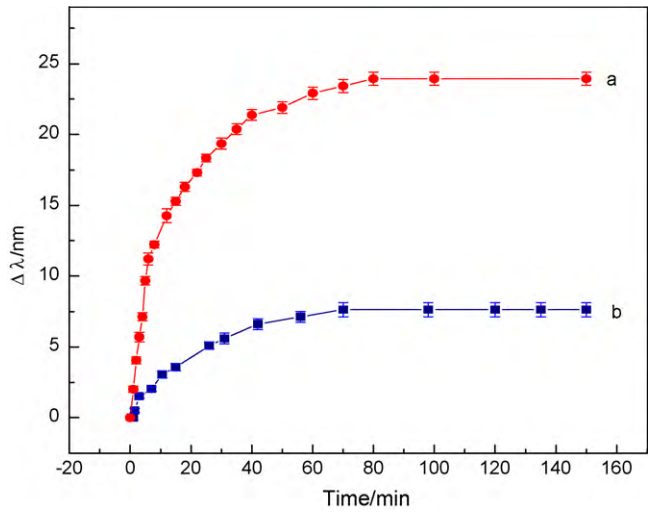

Fig. 7. The kinetic adsorption curves of conjugates of Fe_3O_4/Au nanocomposites coupled with anti-human IgM (a) and anti-human IgM (b).

These experimental results indicated that the biosensor used Fe_3O_4/Au nanocomposites is more sensitive. The exceptional electromagnetic effect of the Au surface plasmon is mostly responsible for improving the biosensor sensitivity. Meanwhile, the Au shell has its own localized surface plasmon due to the collective oscillation of its conduction electrons [31], which would create a stronger local electromagnetic field near the Fe_3O_4/Au nanocomposites. The coupling between the local electromagnetic field of the nanocomposites and Au film could influence the plasmon mode. By this way, the SPR response propagation at the surface of Au film can be increased and the sensitivity of SPR biosensor is enhanced. On the other hand, when the Fe_3O_4/Au nanocomposites were immobilized on the biosensor chip surface, the thickness of the sensing membrane increases and the resonant wavelength moves to longer wavelength, which results in the sensitivity enhancement of the wavelength-modulation SPR biosensor. In conclusion, due to magnetic property and plasmonic property, Fe_3O_4/Au nanocomposites can simplify the immunoassay and improve the sensitivity of SPR biosensor.

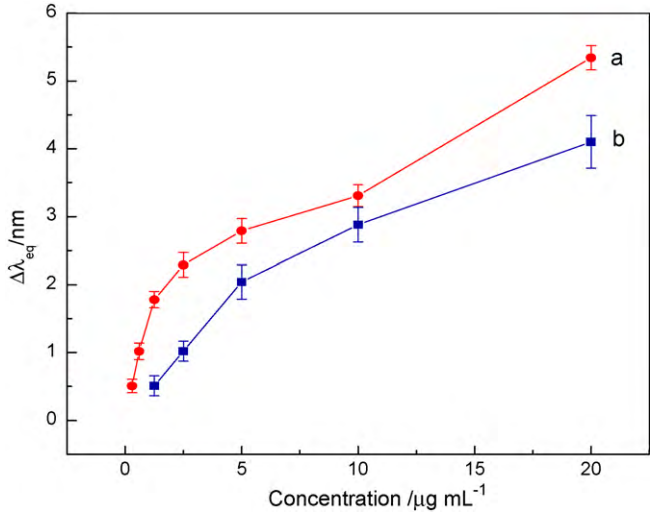

Fig. 8. The relationship between the concentration of human IgM and the shifts of resonant wavelength with the biosensor based on Fe_3O_4/Au nanocomposites (a) and MPA (b). Error bars = ±S.D. and $n = 3$.

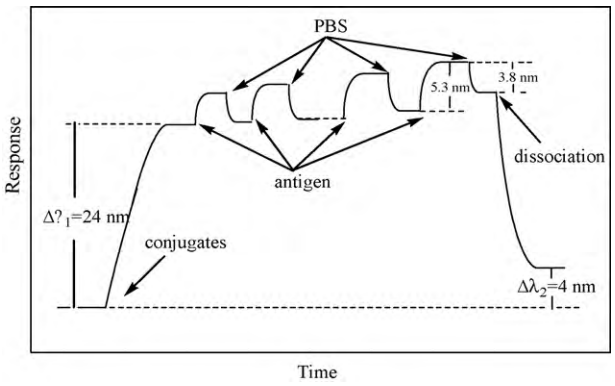

Fig. 9. The SPR response curve of a whole cycle.

3.5. Regeneration of biosensor

The regeneration of biosensor is also an important parameter to affect its practical application. The human IgM at low concentration was detected first. Due to a large amount of ions in the PBS buffer, the antigen could be washed by impulsive injection of PBS buffer [32]. When the concentration is low, the antigen is easy to be removed. The antigen at high concentration, such as 20 μg ml^{-1}, cannot be removed completely (Fig. 9). As the human IgM was detected from low concentration to high concentration, it has little effect on the experimental results.

After the magnetic pillar was taken away from the prism, water was introduced into the flow cell, and the conjugates could be dissociated from the biosensor chip surface. The SPR response curve of the whole cycle is shown in Fig. 9, including the immobilization of conjugates, the binding of antigen at different concentrations and the regeneration of the biosensor. As shown in Fig. 9, the shift of the resonant wavelength of conjugates immobilization is about 24 nm, while the shift of the resonant wavelength of conjugates dissociation is about 20 nm. As the biosensor chip surface is not absolutely smooth, some Fe_3O_4/Au nanocomposites may be immobilized in these pits of surface, which is hard to remove. The dissociation rate of biosensor chip can come up to 83%, which can meet the demand of regeneration. And the biosensor chip can be used repetitive. Traditionally, strong acid or alkali solutions, such as NaOH or HCl solution, were used as regeneration solution to inject the flow cell. After 40 min, the antibodies can be dissociated from the biosensor chip surface. However, the NaOH solution would damage the Au film and reduce the service life of biosensor chip. The use of Fe_3O_4/Au nanocomposites can overcome this limit. In conclusion, the Fe_3O_4/Au nanocomposites are useful to simplify the sensing membrane regeneration procedures.

The evaluation of the selective binding of anti-human IgM was also performed by determining bovine serum albumin and human serum albumin in the concentration range of 5.00–20.00 μg ml^{-1}. The shifts of the resonant wavelength of bovine serum albumin and human serum albumin at 5.00–10.00 μg ml^{-1} were not observable (Fig. 10). When the concentration of bovine serum albumin and human serum albumin is 20 μg ml^{-1}, the resonant wavelength shifted to 0.5 nm. There may be gaps between the conjugates immobilized on the biosensor chip. As a result, the proteins have chance to be immobilized in the gaps, which would induce the non-special adsorption. The shift of the resonant wavelength of 20.00 μg ml^{-1} human IgM is 5.3 nm, which is more obvious than that of non-special adsorption. These experimental results indicated the selective binding of human IgG.

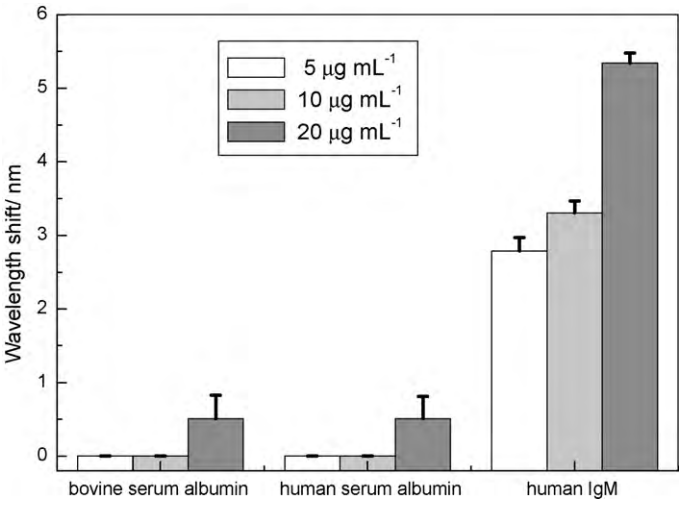

Fig. 10. The shift of resonant wavelength measured by SPR biosensor for different antigens at different concentrations. Error bar = ±S.D. and $n = 3$.

4. Conclusions

The Fe_3O_4/Au nanocomposites modified with MPA, owning good biocompatible and exceptional optical properties, are ideal carriers to bind proteins. And the nanocomposites coupled with proteins can be immobilized on the biosensor chip surface by magnetic pillar easily, which simplifies the procedures of immobilizing proteins and regenerating the sensing membrane. Furthermore, the Fe_3O_4/Au nanocomposites can play an important role in the sensitivity enhancement of SPR biosensor. In this paper, Fe_3O_4/Au nanocomposites coupled with anti-human IgM were immobilized on the surface of SPR biosensor by magnetic pillar to detect human IgM. The experimental results indicate that the decrease of MPA amount results in the increase of nanocomposite diameter, which favors the sensitivity enhancement of SPR biosensor. In addition, the amount of proteins immobilized on the sensing membrane also plays important roles in enhancing the sensitivity of SPR biosensor.

Acknowledgements

This work was supported by National Natural Science Foundation of China (No. 20727003) and Science and Technology Developing Foundation of Jilin Province (No. 20070551).

References

[1] Y.W. Jun, Y.M. Huh, J.S. Choi, J.H. Lee, H.T. Song, S. Kim, S. Yoon, K.S. Kim, J.S. Shin, J.S. Suh, J. Cheon, J. Am. Chem. Soc. 127 (2005) 5732–5733.
[2] S.J. Son, J. Reichel, B. He, M. Schuchman, S.B. Lee, J. Am. Chem. Soc. 127 (2005) 7316–7317.
[3] H. Gu, K.M. Xu, C.J. Xu, B. Xu, Chem. Commun. (2006) 941–949.
[4] D. Caruntu, B.L. Cushing, G. Caruntu, C.J.O. Connor, Chem. Mater. 17 (2005) 3398–3402.
[5] H.W. Gu, R.K. Zheng, X.X. Zhang, B. Xu, J. Am. Chem. Soc. 126 (2004) 5664–5665.
[6] Z.C. Xu, Y.L. Hou, S.H. Sun, J. Am. Chem. Soc. 129 (2007) 8698–8699.
[7] L.Y. Wang, H.Y. Park, S.I. Lim, M.J. Schadt, D. Mott, J. Luo, X. Wang, C.J. Zhong, J. Mater. Chem. 18 (2008) 2629–2635.
[8] G.Y. Shen, H. Wang, G.L. Shen, R.Q. Yu, Anal. Biochem. 365 (2007) 1–6.
[9] J. Bao, W. Chen, T.T. Liu, Y.L. Zhu, P.Y. Jin, L.Y. Wang, J.F. Liu, Y.G. Wei, Y.D. Li, ACS Nano 4 (2007) 293–298.
[10] X.L. Zhao, Y.Q. Cai, T. Wang, Y.L. Shi, G.B. Jiang, Anal. Chem. 80 (2008) 9091–9096.
[11] L.L. Pang, J.S. Li, J.H. Jiang, Y. Le, G.L. Shen, R.Q. Yu, Sens. Actuators B 127 (2007) 311–316.
[12] M. Giersig, P. Mulvaney, Langmuir 9 (1993) 3408–3413.
[13] L. He, E.A. Smith, M.J. Natan, C.D. Keating, J. Phys. Chem. B 108 (2004) 10973–10980.
[14] A.W. Sonesson, T.H. Callisen, H. Brismar, U.M. Elofsson, Colloids Surf. B: Biointerfaces 54 (2007) 236–240.
[15] Y. Teramura, H. Iwata, Anal. Biochem. 365 (2007) 201–207.
[16] Y. Sato, K. Fujimoto, H. Kawaguchi, Colloids Surf. B: Biointerfaces 27 (2003) 23–31.
[17] J. Trevino, A. Calle, J.M. Rodríguez-Frade, M. Mellado, L.M. Lechuga, Talanta 78 (2009) 1011–1016.
[18] V. Chabot, C.M. Cuerrier, E. Escher, V. Aimez, M. Grandbois, P.G. Charette, Biosens. Bioelectron. 24 (2009) 1667–1673.
[19] J. Ladd, H.L. Lu, A.D. Taylor, V. Goodell, M.L. Disis, S.Y. Jiang, Colloids Surf. B: Biointerfaces 70 (2009) 1–6.
[20] X. Liu, Y. Sun, D.Q. Song, Q.L. Zhang, Y. Tian, S.Y. Bi, H.Q. Zhang, Anal. Biochem. 333 (2004) 99–104.
[21] J.L. Wang, A. Munir, Z.H. Li, H.S. Zhou, Biosens. Bioelectron. 25 (2009) 124–129.
[22] S. Sueda, H. Tanaka, M. Yamagishi, Anal. Biochem. 393 (2009) 189–195.
[23] S. Ito, T. Imura, T. Fukuoka, T. Morita, H. Sakai, M. Abe, D. Kitamoto, Colloids Surf. B: Biointerfaces 58 (2007) 165–171.
[24] Y. Sun, Y.P. Bai, D.Q. Song, X.Z. Li, L.Y. Wang, H.Q. Zhang, Biosens. Bioelectron. 23 (2007) 473–478.
[25] E. Fua, S.A. Ramsey, P. Yager, Anal. Chim. Acta 599 (2007) 118–123.
[26] M. Caiazzo, A. Alessandrini, P. Facci, Appl. Mater. Interfaces 1 (2009) 514–525.
[27] D.Q. Song, Y. Mu, X. Liu, L.W. Zhao, H.Q. Zhang, Q.H. Jin, Microchem. J. 74 (2003) 93–97.
[28] S.J. Cho, J.C. Idrobo, J. Olamit, K. Liu, N.D. Browning, S.M. Kauzlarich, Chem. Mater. 17 (2005) 3181–3186.
[29] L.A. Lyon, D.J. Peña, M.J. Natan, J. Phys. Chem. B 103 (1999) 5826–5831.
[30] J. Homola, Sens. Actuators B 41 (1997) 207–211.
[31] L. He, M.D. Musick, S.R. Nicewarner, F.G. Salinas, S.J. Benkovic, M.J. Natan, C.D. Keating, J. Am. Chem. Soc. 122 (2000) 9071–9077.
[32] R. Pei, X. Cui, X. Yang, E. Wang, Talanta 53 (2000) 481–488.